transitions whereas PSII light did not induce state 2. The light independent general ability to perform state transitions indicated that *Stm3* was most likely not affected by a mutation in a gene that is directly connected to the mechanism of state transitions (i.e. LHC kinase/phosphatase activation and regulation system).

LHC-Phosphorylation is Intact in Mutant *Stm3*. *In vivo* LHC phosphorylation rates were studied in *WT* and *Stm3* by immunoblotting with anti-phosphothreonine antibodies. As presented in Fig. 1D, LHC proteins of *WT* and *Stm3* became phosphorylated when intact cells were incubated under state 2 conditions and no differences in the pattern of phosphorylated LHC proteins could be detected. Similar results were obtained *in vitro* using radiolabelled ATP to phosphorylate isolated thylakoid membranes (data not presented). These results clearly indicated that the LHC kinase/phosphatase activation system in *Stm3* is indeed functional.

The Nuclear Gene *nab1* is Disrupted in *Stm3*. Southern blotting analysis confirmed only one integration site of plasmid *pSP124S* in the nuclear genome of *Stm3* (Fig. 2A).

Genetic crosses between *WT* and *Stm3* were performed to test whether the *ble* marker was tightly linked with the *Stm3* phenotype. From these crosses, all clones with phleomycin sensitivity exhibited normal fluorescence phenotype whereas clones showing phleomycin resistance also showed a perturbed state transitions which let us suggest that *Stm3* is a *ble*-tagged mutant.

Initial approaches to determine the site of insertion of plasmid *pSP124S* in *Stm3* by plasmid rescue were not successful because 2.490 bp of the vector DNA including regions necessary for bacterial plasmid amplification and ampicillin resistance were lost in the course of the transformation. Instead LMS-PCR (Strauss et al 2001) was performed to clone endogenous DNA flanking the *ble* cassette in *Stm3*. The success of this method for *Stm3* underlines the fact that LMS-PCR is an important alternative in the analysis of *C. reinhardtii* tagged mutants as it does not rely on an intact transformed vector to identify flanking regions.

2 kb genomic DNA flanking the inserted vector were sequenced (Fig. 2B) and identified as part of an ORF belonging to a putative gene submitted as *nab1* to the databases (Acc.no. AY157846). The gene encodes a protein of mass 26.5 kDa with two predicted RNA binding domains. The function of the gene product is currently being investigated.

To confirm that disruption of *nab1* caused the phenotype in *Stm3*, mutant *Stm3* was successfully complemented in a co-transformation approach using a self-constructed vector containing the endogenous *nab1* gene in combination with a second vector mediating emetine resistance as a dominant selectable marker.

The identification of *nab1* in *C. reinhardtii* underlines the feasibility of our forward genetic approach to identify novel components involved regulating light-driven state transitions.

ACKNOWLEDGMENTS

This work has been supported by the Deutsche Forschungsgemeinschaft (DFG FOR 387).

REFERENCES

Allen, J. F. & Forsberg, J. (2001) *Trends Plant. Sci.* 6: 317–326.

Bonaventura, C. & Myers, J. (1969) *Biochim. Biophys. Acta* 189: 366–386.

Chua, N. H. & Bennoun, P. (1975) *Proc. Natl. Acad. Sci. USA* 72: 2175–2179.

Escoubas, J. M., Lomas, M., Laroche, J. & Falkowski, P. G. (1995) *Proc. Nat. Acad. Sci. USA* 92: 10237–10241.

Haldrup, A., Jensen, P. E., Lunde, C. & Scheller, H. V. (2001) *Trends Plant. Sci.* 6: 301–305.

Kindle, K. L. (1990) *Proc. Natl. Acad. Sci. USA* 87: 1228–1232.

Kruse, O., Nixon, P. J., Schmid, G. H. & Mullineaux, C. W. (1999) *Photosynth. Res.* 61: 43–51.

Laemmli, U. K. (1970) *Nature* 227: 680–685.

Lumbreras, V., Stevens, D. R. & Purton, S. (1998) *Plant J.* 14: 441–448.

Maxwell, D. P., Laudenbach, D. E. & Huner, N. P. A. (1995) *Plant Physiol.* 109: 787–795.

Murata, N. (1969) *Biochim. Biophys. Acta* 172: 242–251.

Sambrook, J., Fritsch, E. F. & Maniatis, T. (1989) in: Molecular Cloning (N. Ford, C. Nolan & M. Ferguson, Eds.) Cold Spring Harbor Laboratory Press, NY.

Stevens, D. R., Rochaix, J. D. & Purton, S. (1996) *Mol. Gen. Genet.* 251: 23–30.

Strauss, C., Mussgnug, J. H. & Kruse, O. (2001) *Photosynth. Res.* 70: 311–320.

Yang, D. H., Andersson, B., Aro, E. M. & Ohad, I. (2001) *Photosynth. Res.* 68: 63–174.

ROLE OF *ANABAENA* FLAVODOXIN HYDROPHOBIC RESIDUES IN PROTEIN-PROTEIN INTERACTION AND ELECTRON TRANSFER TO FERREDOXIN-NADP$^+$ REDUCTASE

Susana Frago[1], Guillermina Goñi[1], Ana Serrano[1], Stephen G. Mayhew[2], Carlos Gómez-Moreno[1], Milagros Medina[1]. [1]Departamento de Bioquímica y Biología Molecular y Celular and Instituto de Biocomputación y Física de Sistemas Complejos, Facultad de Ciencias. Universidad de Zaragoza. 50009-Zaragoza. Spain. [2]Department of Biochemistry. Conway Institute for Biomolecular and Biomedical Research, University College Dublin. Belfield. Dublin 4. Ireland

Keywords: flavodoxin, ferredoxin-NADP$^+$ reductase, protein-protein interaction, electron transfer

INTRODUCTION

Biochemical and structural studies indicate that electrostatic and hydrophobic interactions play an important role in formation of optimal complexes for efficient electron transfer between ferredoxin-NADP$^+$ reductase (FNR) and ferredoxin (Fd) (Medina et al 2004). Moreover, it has been shown that several charged and hydrophobic residues on the FNR surface are also critical for the interaction with flavodoxin (Fld) (Medina et al 2004), although, so far, no key residue on the Fld surface has been found to be the counterpart of FNR side-chains (Casaus et al 2002, Nogués et al 2003). In this study, side-chains with a hydrophobic character on the *Anabaena*

Fld surface have been modified. Thus, the W57R, W57K, W57E, I59E/I92E and I59A/I92A Fld mutants have been produced and their binding and electron transfer abilities with FNR evaluated. Taking into account the role played by the residues in the 50's and the 90's loops in Fld in the modulation of the redox properties of the bound FMN redox cofactor (Swenson et al 1994, Zhou et al 1996, Lostao et al 1997) the midpoint reduction potentials of these mutants have been determined.

MATERIALS AND METHODS

Biological material. Site-directed mutagenesis to produce *Anabaena* PCC7119 Fld mutants was carried out by using the QuickChange mutagenesis kit and suitable synthetic oligonucleotides. Mutations were verified by DNA sequence analysis. The expression and purification of the Fld mutants was as described previously (Lostao et al 1997).

Spectroscopic analysis. UV/Vis spectra of Flds were recorded on a Kontron Uvikon 942 or on a CARY 1. Dissociation constants and binding energies for the complexes between WT FNR_{ox} and the different Fld_{ox} forms were obtained by differential spectroscopy (Medina et al 1998, Nogués et al 2003). Fitting the experimental data to the theoretical equation for a 1:1 complex allowed the calculation of K_d and $\Delta\varepsilon$. Errors in the estimated values were ±15 %. The FNR-dependent NADPH-cytochrome *c* reductase activity was assayed using the different Fld mutants as the electron carrier from FNR to cytochrome *c* (Medina et al 1998, Nogués et al 2003). Errors in the estimated K_m and k_{cat} values were ±15% and ±10% respectively. Unless otherwise stated all measurements were carried out at 25 °C in 50 mM Tris/HCl, pH 8.0.

Reduction potential determinations. Midpoint reduction potentials of Fld mutants were determined by anaerobic photoreduction in the presence of 1 μM dRf and 2 mM EDTA at 25 °C using a saturated calomel electrode as reference (Mayhew 1999). Solutions were made anaerobic by several cycles of evacuation and flushing with O_2-free N_2. Stepwise Fld photoreduction was achieved by irradiating the solution with a 250 W lamp for periods of approximately 1 min. The solution potential was monitored using a Sycopel Ministat potentiostat. Equilibration of the system was considered established when the measured potential remained stable for 20 min, and the UV–Vis spectrum was then recorded. The concentrations of the different redox species in equilibrium were determined from the absorbance spectra. The midpoint potentials for the redox couples were calculated by linear regression analysis of plots of potential versus logarithm of concentration ratio (oxidised/semiquinone or semiquinone/hydroquinone) according to the Nernst equation,

$$E = E_m + (0.059/n)\log([ox]/[rd]) \quad (1)$$

The midpoint potentials are reported relative to the potential of the standard hydrogen electrode. Typical experimental solutions contained 25–40 μM protein, 1–3 μM indicator dyes, 1 μM dRf and 2 mM EDTA at 25 °C. The following dyes were used as mediators: 1 μM anthraquinone-2,6-disulfonate and 1 μM anthraquinone-2-sulfonate for the determination of $E_{ox/sq}$; 1 μM benzyl viologen and 1 μM methyl viologen for the determination of $E_{sq/rd}$. Error in the $E_{ox/sq}$ and $E_{sq/red}$ was estimated ±5 mV.

RESULTS

Reduction Potentials. Redox titration of the different Fld mutants allowed Nernst plots representations for $E_{ox/sq}$ and $E_{sq/rd}$ (Fig. 1, Table 1). In general, although both midpoint reduction potentials change for the mutants with regard to the WT Fld, larger effects are seen in $E_{ox/sq}$ (−72 to +76 mV) than in $E_{sq/rd}$ (+49 mV). The effects are different for the mutants at position of W57 and the double mutants at I59/I92. Replacement of W57 by a positively charged side-chain makes both $E_{ox/sq}$ and $E_{sq/rd}$ less negative, whereas much more moderate effects are observed in W57E. In all these mutants only a small decrease in the maximal amount of stabilised semiquinone is observed.

However, simultaneous replacement of I59 and I92 by either Glu or Ala considerably shifts the $E_{ox/sq}$ to more negative values and the $E_{sq/rd}$ to less negative. Thus, in these two mutants the potentials for the two steps tend to converge so that the semiquinone that is stabilised decreases from 97% for WT Fld to 82% and only 61% for I59E/I92E and I59A/I92A, respectively (Table 1).

Steady-State Kinetics Analysis of the Different Fld Mutants. k_{cat} values obtained for FNR when using the different Fld mutants as electron carriers in the Fld-mediated NADPH-dependent cytochrome *c* reductase assay for the W57E, I59E/I92E and I59A/I92A were 1.5-fold lower than those reported when using WT Fld (Table 2). However, introduction of positively charged residues at position W57 produced a considerable increment of the enzyme turnover. More noticeable are the effects observed in the FNR K_m values, since all the mutations introduced at position 57 considerably increase this parameter (up to a factor of 3-fold), suggesting a

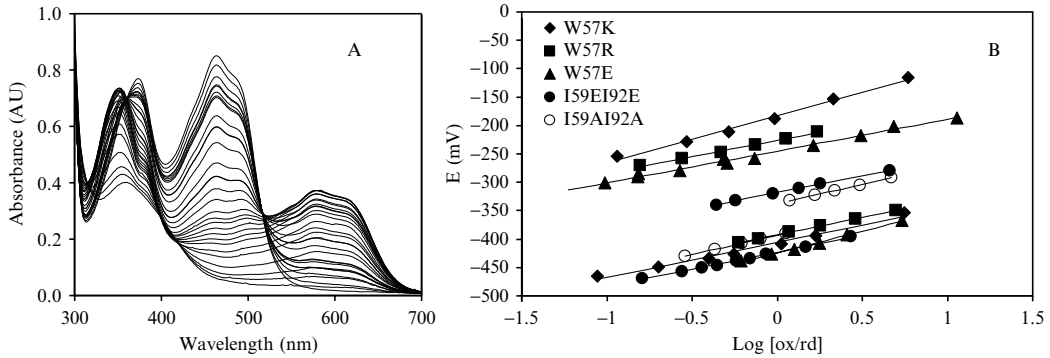

Figure 1: (A) UV–Visible spectra obtained during redox titration of I59E/I92E Fld, 25 °C, Tris/HCl 50 mM, pH 8.0. (B) Oxidised/semiquinone and semiquinone/reduced Nernst plots for the different Fld forms.

Table 1: Midpoint reduction potentials and percentage of maximal semiquinone stabilised for the different Fld forms

Fld Form	$E_{ox/sq}$ (mV)	$E_{sq/rd}$ (mV)	% sq
WT[a]	−266	−439	97
W57K	−190	−410	96
W57E	−253	−421	93
W57R	−227	−391	91
I59E/I92E	−317	−423	82
I59A/I92A	−338	−423	61

[a] Data from Nogués et al (2003).

Table 2: NADPH-dependent cytochrome *c* reductase activity of WT FNR with different mutated flavodoxins as mediator in the FNR NADPH-cytochrome *c* reductase assay and dissociation constants and $\Delta\varepsilon_{(462\,nm)}$ for complex formation of oxidised WT *Anabaena* FNR with WT and mutated flavodoxin forms

Fld Form	k_{cat}^{Fld} (s^{-1})	K_m^{Fld} (μM)	k_{cat}/K_m^{Fld} ($\mu M^{-1} s^{-1}$)	K_d (μM)	$\Delta\varepsilon_{(462\,nm)}$ ($mM^{-1} cm^{-1}$)
WT[a]	23.3	33.0	0.70	3.0	1.4
W57K	90.3	89.1	1.01	31.0	2.0
W57E	13.8	70.1	0.20	>50	—
W57R	52.7	76.7	0.69	19.7	1.4
I59E/I92E	14.0	40.0	0.35		
I59A/I92A	15.3	33.8	0.45		

[a] Data from Medina et al (1998).

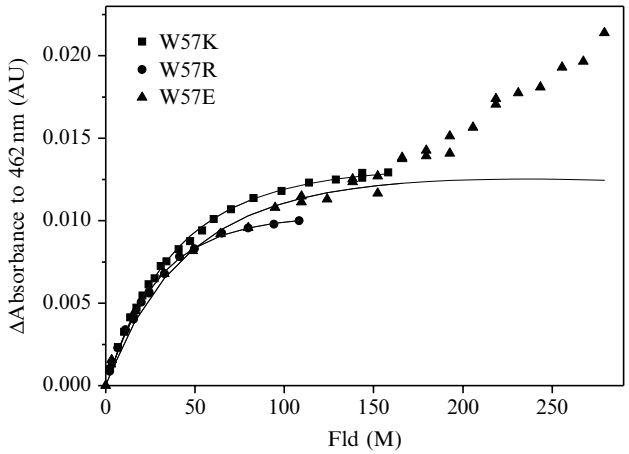

Figure 2: Spectrophotometric titration (ΔAbs 462 nm) of FNR_{ox} forms with the W57 Fld_{ox} mutants. Solid lines fitted for the formation of a 1:1 complex.

weaker interaction, whereas the value remains similar to that of WT for the I59E/I92E and I59A/I92A variants. Taking into account these parameters it turned out that the catalytic efficiency (k_{cat}/K_m) of FNR when using the different Fld variants was slightly lower for W57E, I59E/I92E and I59A/I92A Flds, whereas slightly increased for the W57K variant.

Interaction of Fld_{ox} Variants with WT FNR_{ox}. The visible difference spectrum of the WT Fld_{ox}:FNR_{ox} complex has been proposed to arise from alteration of the FNR flavin environment upon Fld association, and shows absorption maxima around 390 and 464 nm (Medina et al 1998, Casaus et al 2002). Similar spectral perturbations are obtained for the complexes between FNR_{ox} and all the Fld_{ox} mutants at the W57 position (not shown), indicating that upon complex formation the FNR flavin environment is altered to the same extent with the mutants than with the WT Fld. With regard to the calculated K_d values for the FNR_{ox}:Fld_{ox} complex, greater values were obtained for the mutants, suggesting a weaker interaction upon replacement of W57. Additionally, titration of FNR_{ox} with W57E Fld_{ox} does not show the typical saturation behaviour for a 1:1 interaction (Fig. 2), and the linear dependence observed suggest formation of non-specific interactions.

DISCUSSION

Replacement of W57 by a polar side-chain considerably weakens the FNR:Fld interaction. However, whereas introduction of a negative side-chain produces a deleterious effect in the Fld ability to accept electrons from FNR, a positively charged side-chain produces a more efficient Fld in this process. This later observation can be explained because introduction of a positively charged side-chain at position 57 produces Flds with less negative reduction potentials while the W57E mutant produces non-specific FNR:Fld associations. Therefore, the I59 and I92 side-chains are not key residues for the interaction of *Anabaena* Fld with FNR. However, the side-chains of these residues modulate the FMN reduction potentials and the ability of Fld to function as electron transfer protein.

In conclusion, although Trp57, Ile59 and Ile92 side-chains are not involved in the formation of individually crucial interactions with FNR, they all contribute to the interaction perhaps by providing optimal orientation. Additionally, these residues, situated in the close environment of the FMN isoalloxazine ring, modulate the flavin reduction properties within the protein environment. Therefore, their side-chains contribute to both modulation of the oxidation-reduction properties of Fld and its ability to bind to and exchange electrons.

ACKNOWLEDGMENTS

This work has been supported by Comisión Interministerial de Ciencia y Tecnología (BQU2001-2520 to M.M.).

REFERENCES

Casaus, J. L., Navarro, J. A., Hervás, M., Lostao, A., de la Rosa, M. A., Gómez-Moreno, C., Sancho, J. & Medina, M. (2002) *J. Biol. Chem.* 277: 22338–22344.

Lostao, A., Gomez-Moreno, C., Mayhew, S. G. & Sancho, J. (1997) *Biochemistry* 36: 14334–14344.

Mayhew, S. G. (1999) in: Flavoprotein Protocols (S. K. Chapman & G. A. Reid, Eds.) pp. 49–59. Humana Press, Totowa, New Jersey.

Medina, M. & Gómez-Moreno, C. (2004) *Photosynth. Res.* 79: 113–131.

Medina, M., Martínez-Júlvez, M., Hurley, J. K., Tollin, G. & Gómez-Moreno, C. (1998) *Biochemistry* 37: 2715–2728.

Nogués, I., Martínez-Júlvez, M., Navarro, J. A., Hervás, M., de la Rosa, M. A., Gómez-Moreno, C. & Medina, M. (2003) *Biochemistry* 42: 2036–2045.

Swenson, R. P. & Krey, G. D. (1994) *Biochemistry* 33: 8505–8514.

Zhou, Z. & Swenson, R. P. (1996) *Biochemistry* 35: 15980–15988.